Quantum point contacts as a subject of the theory of quantum size effects

2009 J. Phys. A: Math. Theor. 42 055206

(http://iopscience.iop.org/1751-8121/42/5/055206)

IOP PUBLISHING JOURNAL OF PHYSICS A: MATHEMATICAL AND THEORETICAL

J. Phys. A: Math. Theor. **42** (2009) 055206 (19pp) doi:10.1088/1751-8113/42/5/055206

Quantum point contacts as a subject of the theory of quantum size effects

Viktor Bezák

Department of Experimental Physics, Comenius University, 84248 Bratislava, Slovakia

E-mail: bezak@fmph.uniba.sk

Received 9 July 2008, in final form 13 November 2008
Published 6 January 2009
Online at stacks.iop.org/JPhysA/42/055206

Abstract

Detailed calculations are carried out demonstrating conductance quantization with a 2D quantum point contact (QPC). The QPC is defined as a gap of width a in a diaphragm located perpendicularly in a narrow stripe of width L_x. The stripe is considered as a container of an ideal gas of electrons at zero temperature. Emphasis is put on treating the stripe as a quantum-mechanical waveguide of the electrons. For simplicity, collisions of the electrons inside the stripe are neglected. The author focuses attention on the dependence of the conductance of the QPC on the variable $u = ak_F$. ($\hbar k_F$ is the Fermi momentum.) The plot of this dependence exhibits steps manifesting two kinds of singular points. The frontal edge of each conductance step represents a singularity of the type $\sim 1/\sqrt{u - u_\mu}$. This corresponds to the singularity of the type $\sim 1/(n_e - n_{e\mu})$ when the density n_e of the electrons is used rather than the variable u. (If collisions of the electrons inside the stripe are taken into account, this singularity is transformed into a sharp finite-value maximum.) The second kind of singularity is of the type $\sim\sqrt{u - u_v}$ and is due to the waveguide character of the stripe. The author exemplifies his theory with a configuration defined with the gap ratio $a/L_x = 1/2$.

PACS numbers: 03.65.Nk, 05.60.Gg, 61.05.jm, 73.40.Cg, 73.63.Rt

1. Introduction

Solid state physicists used to speak of size effects usually in connection with studying the dependence of transport parameters of metallic or semiconductor thin films on their thickness. As a rule, nowadays we distinguish between classical and quantum size effects, the first concerning films with thicknesses comparable with the mean free path of conduction electrons [1], and the second concerning much thinner films, such films whose thickness is comparable with the mean de Broglie wavelength of the conduction electrons. As the

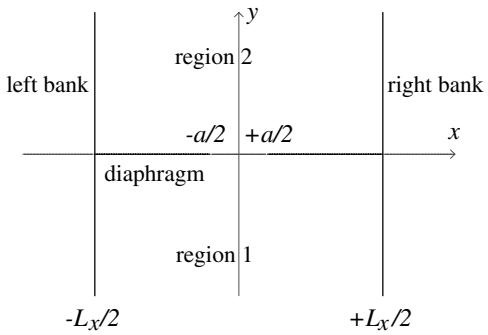

Figure 1. Scheme of the stripe with the diaphragm. The gap in the diaphragm of width a is the QPC, regions 1 and 2 are leads to it.

wavelength $\lambda_F = 2\pi/k_F$ corresponding to the Fermi momentum $\hbar k_F$ in metals is of the order of magnitude of atomic radii, the quantum size effects were studied preferably with semi-metallic (such as bismuth) films [2], or with degenerate semiconductor (such as n-InSb) films [3, 4], where λ_F can be by 2–3 orders of magnitude greater than in metals. The literature about the quantum size effects is enormous, cf, e.g. the review article [5] published in 1982. Since then, many observations of quantum size effects were reported.

When an ideal electron gas is confined between impenetrable parallel walls that are a given distance L_x apart, we can imagine standing de Broglie waves with k_x equal to $\pm\pi\nu/L_x$ ($\nu = 1, 2, \ldots$) This means that when considering a given density of the electrons n_e at $T = 0$, we may speak of 'Fermi disks' instead of the Fermi sphere (which is the usual concept in case of bulk metallic samples). Employing the well-known Sommerfeld model, we may interpret L_x as the thickness of a metallic film, or an n-type InSb film. In our early paper [3], we have derived the dependence of the Fermi energy on the thickness L_x, showing that this dependence resembled damped oscillations. These oscillations were of a non-harmonic type: there were jags at points of local maxima and we could clarify each jag as the onset of a new pair of disks inside the Fermi sphere when the thickness L_x increased. (The radius k_F of the Fermi sphere was thickness dependent, although the density n_e was kept constant.)

In the present paper, we will return to the idea presented in [3], but now considering its 2D analogy. In the case that we will treat, we will not have in mind a 3D electron gas between parallel planes, but a 2D electron gas between parallel straight lines. Thus, instead of a thin layer, now we will consider a stripe on a plane, assuming that L_x is the width of this stripe. Moreover, we will consider a diaphragm in the stripe, as is shown in figure 1. We call the gap in the diaphragm the quantum point contact (QPC). The lower and upper part of the stripe are actually leads to the QPC. In 1988, two groups [6, 7] published results of measurements with 2D QPCs (although designed with a geometry different from that shown in figure 1) and corroborated excellently the phenomenon of the conductance quantization. Afterwards, during the last two decades, many theoretical papers emerged so that now we may state that various problems connected with this phenomenon were clarified in detail [8–19]. As a rule, the authors of these papers directed their analysis on quantum-mechanical consequences following from the geometrical constriction defining the QPC as such, but did not pay attention to the leads to the QPC from the quantum-mechanical viewpoint. Instead, they either treated electrons in the leads quasi-classically, or did not pay attention to the leads at all. However, if the leads are sufficiently narrow, they should necessarily be treated as quantum-mechanical

waveguides. Therefore, when theorizing about a QPC, it is indispensable to deal with the system 'QPC+leads' as with a whole. The model suggested by the scheme in figure 1 defines a quantum-mechanical problem which is exactly solvable. How to derive the solution of this problem is the proper objective of the present paper.

2. Mathematical preliminaries

We will solve the Schrödinger equation describing the 2D motion of electrons in a stripe of a given width L_x. We define the boundaries of the stripe as the straight lines $x = \pm L_x/2$. The problem with which we intend to deal is the scattering of electrons on a diaphragm laid perpendicularly across the stripe (figure 1). We lay the diaphragm, assuming that its thickness is zero, on the x-axis. We consider the lower (upper) half of the stripe, defined by the inequality $y < 0$ ($y > 0$), as region 1 (region 2). Correspondingly, we write the wavefunction of an electron as $\psi^{(\tau)}(x, y) \equiv \psi^{(\tau)}(\mathbf{r})$ with $\tau = 1$ if $y < 0$ and $\tau = 2$ if $y > 0$. ($\mathbf{r}$ is the 2D position vector.) Neglecting the potential energy due to scatterers of electrons inside the regions 1 and 2, we may write the equations

$$\begin{aligned} &\nabla^2\psi^{(1)}(\mathbf{r}) + k^2\psi^{(1)}(\mathbf{r}) = 0 \qquad \text{for} \quad y < 0, \\ &\nabla^2\psi^{(2)}(\mathbf{r}) + k^2\psi^{(2)}(\mathbf{r}) = 0 \qquad \text{for} \quad y > 0, \end{aligned} \tag{1}$$

where

$$k = \sqrt{2m\mathcal{E}}/\hbar > 0. \tag{2}$$

$\mathcal{E} > 0$ is the one-electron energy. We consider the regions 1 and 2 as (quasi)metallic leads and interpret them as reservoirs of a gas of non-interacting electrons at $T = 0$. Equations (1) correspond to the parabolic dispersion law

$$\mathcal{E} = \frac{\hbar^2\left(k_x^2 + k_y^2\right)}{2m} \tag{3}$$

of the conduction electrons in the leads, with a scalar effective mass $m > 0$.

We define the diaphragm with a window of width a centered at $x = 0$. Then we postulate the boundary conditions

$$\begin{aligned} &\psi^{(1)}(L_x/2, y) = \psi^{(1)}(-L_x/2, y) = 0 \qquad \text{for} \quad y < 0, \\ &\psi^{(2)}(L_x/2, y) = \psi^{(2)}(-L_x/2, y) = 0 \qquad \text{for} \quad y > 0 \end{aligned} \tag{4}$$

and

$$\begin{aligned} &\psi^{(1)}(x, -0) = 0 \qquad \text{for} \quad a/2 < |x| < L_x/2, \\ &\psi^{(2)}(x, +0) = 0 \qquad \text{for} \quad a/2 < |x| < L_x/2. \end{aligned} \tag{5}$$

In the window, we postulate the continuity of the wavefunction and of its derivative with respect to y

$$\left.\begin{aligned} &\psi^{(1)}(x, -0) = \psi^{(2)}(x, +0) \\ &\partial\psi^{(1)}(x, y)/\partial y|_{z=-0} = \partial\psi^{(2)}(x, y)/\partial y|_{z=+0} \end{aligned}\right\} \qquad \text{for} \quad -a/2 < x < a/2. \tag{6}$$

The motion of the conduction electrons is quantized in the x-direction. We write

$$\mathcal{E}_\nu^x(L_x) = \frac{\hbar^2}{2m}\left(\frac{\pi\nu}{L_x}\right)^2 \qquad \nu = 1, 2, \ldots. \tag{7}$$

The energy $\mathcal{E}_\nu^x(L_x)$ is doubly degenerated, as the electrons may travel towards the diaphragm either in the positive or in the negative direction of the y-axis. Respectively, we may speak of states $|\nu\rangle_+$ and $|\nu\rangle_-$. From now on, we will focus attention on states $|\nu\rangle_+$.

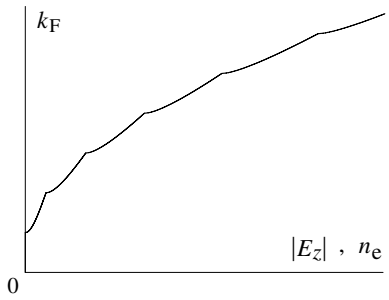

Figure 2. If a suitable scale is used, this figure shows the dependence of k_F on n_e or on $|E_z|$.

Let $\mathcal{E}_F$ be the Fermi energy of the conduction electrons at $T = 0$, and let $\hbar k_F$ be the Fermi momentum

$$k_F = \sqrt{2m\mathcal{E}_F}/\hbar. \tag{8}$$

With a fixed value of the width a of the window, we may employ

$$u = k_F a \tag{9}$$

as a suitable dimensionless variable. Since we consider the parabolic dispersion law, the energy $\mathcal{E}$ for any value of $|\mathbf{k}| = k$ is a sum of contributions due to the motion in the x- and y-directions. Therefore, we define the energy difference

$$\mathcal{E}_\nu^y(L_x) = \mathcal{E} - \mathcal{E}_\nu^x(L_x), \tag{10}$$

which we write as $\mathcal{E}_{F,\nu}^y(L_x)$ if $\mathcal{E} = \mathcal{E}_F$. We define also the positive variable

$$k_\nu^y(L_x) = \sqrt{2m\mathcal{E}_\nu^y(L_x)}/\hbar = \sqrt{k^2 - \pi^2\nu^2/L_x^2} \tag{11}$$

if $\mathcal{E}_\nu^y(L_x) > 0$ (i.e. if $k > \pi\nu/L_x$), which we write as $k_{F,\nu}^y(L_x)$ if $k = k_F$. Clearly, values of k that are smaller than π/L_x are forbidden.

As is well known, the 2D electron gas can be realized near to a planar surface of a direct-gap semiconductor (such as GaAs) if a strong perpendicular electrical field E_z is applied. (We define the surface as the plane $z = 0$.) If the field E_z is suitably adjusted, it attracts a 'cloud' of electrons near to the surface. When neglecting the intrinsic surface charge due to quantum-mechanical surface states, we may state that the density n_e of the electrons (i.e. their number per unit area of the surface) is equal (according to the Poisson equation of electrostatics) to $e|E_z|/\epsilon$. (ϵ is the permittivity of the semiconductor.) Thus the field E_z can control the value of the density of the electrons n_e. However, we may also use k_F as a variable that can be controlled by the external field E_z. This possibility is based on the fact that there is a one-to-one correspondence between k_F and n_e (cf figure 6 in the appendix).

Figure 2 is the inversion of figure 6. Since the variables u and F used in the appendix are proportional to k_F and n_e, respectively, figure 2 may be interpreted as the dependence of the variable k_F on the electron density n_e or (as n_e is proportional to E_z) also as the dependence of k_F on the perpendicular electrical field E_z. The presence of the 'jags' (although they are obtuse) in the curve shown in figure 2 is actually a manifestation of a quantum size effect in the sense suggested in the introduction. Indeed, if we consider, instead of one stripe, an ensemble of stripes with various widths L_x and stipulate the constancy of the density n_e of the electrons in all the stripes, then we can easily transform the plot shown in figure 2 into a

plot that will correspond to the dependence of k_F on L_x. In the limiting case, we obtain the well-known result for the 2D electron gas that is not confined in the x-direction

$$\lim_{L_x\to\infty} k_F = \sqrt{2\pi n_e}. \tag{12}$$

The curve in figure 2 essentially follows this dependence, but is perturbed by the 'jags'.

Now we can specify the objectives of the present paper. In section 3, we will derive the exact solution of the Schrödinger equation for the QPC plus the leads corresponding to the scheme shown in figure 1. Afterwards, in section 4, we will calculate the conductance of this QPC.

3. Solution of the Schrödinger equation

Having in mind figure 1, we consider an electron impacting with $k_\nu^y(L_x)$ from the side of region 1 upon the diaphragm. The value of ν is an arbitrary positive integer, $\nu = 1, 2, \ldots$. The corresponding incident wavefunction $\psi_\nu^{(0)}(\mathbf{r})$ may be either even or odd in the variable x

$$\psi_\nu^{(0)}(\mathbf{r}) = \begin{cases} N_\nu \sqrt{\dfrac{2}{L_x}} \cos\left(\dfrac{\pi\nu x}{L_x}\right) \exp\left[\mathrm{i}k_\nu^y(L_x)y\right] & \text{if} \quad \nu \text{ is odd,} \\ N_\nu \sqrt{\dfrac{2}{L_x}} \sin\left(\dfrac{\pi\nu x}{L_x}\right) \exp\left[\mathrm{i}k_\nu^y(L_x)y\right] & \text{if} \quad \nu \text{ is even.} \end{cases} \tag{13}$$

N_ν is a real normalizing coefficient; we will define it later on (cf formula (30)). In the style of a scattering theory, we introduce the wavefunctions $\chi_\nu^{(\tau)}(x, y) = \chi_\nu^{(\tau)}(x, y)(\mathbf{r})$ $(\tau = 1, 2)$

$$\begin{aligned} \psi_\nu^{(1)}(\mathbf{r}) &= \psi_\nu^{(0)}(\mathbf{r}) + \chi_\nu^{(1)}(\mathbf{r}), \qquad y < 0, \\ \psi_\nu^{(2)}(\mathbf{r}) &= \chi_\nu^{(2)}(\mathbf{r}), \qquad y > 0. \end{aligned} \tag{14}$$

3.1. Autonomous derivation of the functions $\chi_\nu^{(1)}(x, -0) = \chi_\nu^{(2)}(x, +0)$ and $\partial\chi_\nu^{(1)}(\mathbf{r})/\partial z\big|_{y=-0} = \partial\chi_\nu^{(2)}(\mathbf{r})/\partial z\big|_{y=+0}$ in the window $(-a/2 < x < a/2)$

We will now discuss the solution of the Schrödinger equation in a narrow oblong with bases $y = \pm\epsilon/2$ and with sides $x = \pm a/2$, assuming that the thickness $\epsilon > 0$ of this oblong is very small, $\epsilon \ll a$. We introduce the orthonormal set of the functions, indexed by $\mu = 1, 2, \ldots$ and defined for $x \in (-a/2, a/2)$,

$$\varphi_\mu(x) = \begin{cases} \sqrt{\dfrac{2}{a}} \cos\left(\dfrac{\pi\mu x}{a}\right), & \mu = \text{odd}, \\ \sqrt{\dfrac{2}{a}} \sin\left(\dfrac{\pi\mu x}{a}\right), & \mu = \text{even}. \end{cases} \tag{15}$$

Correspondingly we define the lateral energy values

$$\mathcal{E}_\mu^x(a) = \frac{\hbar^2}{2m}\left(\frac{\pi\mu}{a}\right)^2 \qquad \mu = 1, 2, \ldots \tag{16}$$

and the energy differences

$$\mathcal{E}_\mu^y(a) = \mathcal{E} - \mathcal{E}_\mu^x(a). \tag{17}$$

We say that μ enumerates possible QPC modes, or synonymously QPC 'channels'. We use the denotation

$$k_\mu^y(a) = \begin{cases} \sqrt{2m\mathcal{E}_\mu^y(a)}/\hbar = \sqrt{k^2 - \pi^2\mu^2/a^2} > 0 & \text{if} \quad \mathcal{E}_\mu^y(a) > 0, \\ \sqrt{2m|\mathcal{E}_\mu^y(a)|}/\hbar = \sqrt{\pi^2\mu^2/a^2 - k^2} > 0 & \text{if} \quad \mathcal{E}_\mu^y(a) < 0. \end{cases} \tag{18}$$

Let $\mathcal{M}(k) \geqslant 1$ be the maximum value of the index μ for which $k > \pi\mathcal{M}(k)/a$. Then, for $x \in (-a/2, a/2)$, we express $\chi_\nu^{(\tau)}(x, y)$ as the series

$$\begin{aligned}
\chi_\nu^{(1)}(x, y) \equiv \Omega_\nu^{(1)}(x, y) &= \sum_{\mu=1}^{\mathcal{M}(k)} r_\nu^\mu \varphi_\mu(x) \exp\left[-\mathrm{i}k_\mu^y(a)y\right] \\
&+ \sum_{\mu=\mathcal{M}(k)+1}^{\infty} r_\nu^\mu \varphi_\mu(x) \exp\left[+\kappa_\mu^y(a)y\right], \qquad y \in (-\epsilon/2, 0), \\
\chi_\nu^{(2)}(x, y) \equiv \Omega_\nu^{(2)}(x, y) &= \sum_{\mu=1}^{\mathcal{M}(k)} t_\nu^\mu \varphi_\mu(x) \exp\left[+\mathrm{i}k_\mu^y(a)y\right] \\
&+ \sum_{\mu=\mathcal{M}(k)+1}^{\infty} t_\nu^\mu \varphi_\mu(x) \exp\left[-\kappa_\mu^y(a)y\right], \qquad y \in (0, \epsilon/2).
\end{aligned} \tag{19}$$

(Of course, μ at 'r' and 't' is to be read as a superscript, not as a power.) For $x \in (-a/1, a/2)$, we write also the series

$$\begin{aligned}
\sqrt{\frac{2}{L_x}} \cos\left(\frac{\pi\nu x}{L_x}\right) &= \sqrt{\frac{2}{a}} \sum_{\mathrm{odd}\mu>0} c_\nu^\mu \cos\left(\frac{\pi\mu x}{a}\right) \qquad \text{if} \quad \nu \text{ is odd}, \\
\sqrt{\frac{2}{L_x}} \sin\left(\frac{\pi\nu x}{L_x}\right) &= \sqrt{\frac{2}{a}} \sum_{\mathrm{even}\mu>0} c_\nu^\mu \sin\left(\frac{\pi\mu x}{a}\right) \qquad \text{if} \quad \nu \text{ is even}.
\end{aligned} \tag{20}$$

For formal reasons, we deem it useful to define the dimensionless parameter

$$\gamma = a/L_x \tag{21}$$

which we call the *gap ratio*. (It is the ratio between the width of the window in the diaphragm and the width of the leads.) The maximum value of the gap ratio, $\gamma_{\max} = 1$, corresponds to the absence of the diaphragm. On the other hand, $\gamma_{\min} = 0$ corresponds to the absence of the window in the diaphragm.

The Fourier analysis gives us the coefficients

$$c_\nu^\mu = \begin{cases} 2\sqrt{\gamma}\left[\dfrac{\sin[(\pi/2)(\mu-\nu\gamma)]}{\mu-\nu\gamma} + \dfrac{\sin[(\pi/2)(\mu+\nu\gamma)]}{\mu+\nu\gamma}\right] & \text{if} \quad \text{both } \mu, \nu \text{ are odd}, \\ 2\sqrt{\gamma}\left[\dfrac{\sin[(\pi/2)(\mu-\nu\gamma)]}{\mu-\nu\gamma} - \dfrac{\sin[(\pi/2)(\mu+\nu\gamma)]}{\mu+\nu\gamma}\right] & \text{if} \quad \text{both } \mu, \nu \text{ are even}. \end{cases} \tag{22}$$

Otherwise $c_\nu^\mu = 0$.

Our primary objective is to calculate the one-electron current density

$$j_2^{(1\mathrm{e})}(x, y) = \frac{\mathrm{i}e\hbar}{2m}\left(\psi^{(2)*}(\mathbf{r})\frac{\partial\psi^{(2)}(\mathbf{r})}{\partial y} - \psi^{(2)}(\mathbf{r})\frac{\partial\psi^{(2)*}(\mathbf{r})}{\partial y}\right) \tag{23}$$

for $y \to +0$. This is equal to

$$j_1^{(1\mathrm{e})}(x, y) = \frac{\mathrm{i}e\hbar}{2m}\left(\psi^{(1)*}(\mathbf{r})\frac{\partial\psi^{(1)}(\mathbf{r})}{\partial y} - \psi^{(1)}(\mathbf{r})\frac{\partial\psi^{(1)*}(\mathbf{r})}{\partial y}\right) \tag{24}$$

for $y \to -0$. The incident wavefunction $\psi_\nu^{(0)}(\mathbf{r})$ gives rise to the (one-electron) electrical current through the window in the diaphragm

$$J_\nu^{(1\mathrm{e})}(k) = \int_{-a/2}^{a/2} \mathrm{d}x\, j_{2\nu}^{(1\mathrm{e})}(x, +0) = \int_{-a/2}^{a/2} \mathrm{d}x\, j_{1\nu}^{(1\mathrm{e})}(x, -0). \tag{25}$$

Recalling formulae (14) and employing series (19) in formulae (23), (24), we find (when respecting the orthonormality of the functions $\varphi_{(\mathrm{e,o})\mu}(x)$) that the current is equal to the sum

$$J_\nu^{(1\mathrm{e})}(k) = -\frac{e\hbar}{m}\sum_{\mu=1}^{\mathcal{M}(k)} \left|t_\nu^\mu\right|^2 k_\mu^y(a). \tag{26}$$

This formula indicates that we need not consider the evanescent waves involved in expressions (19). Since μ is the serial number of the channel into which the wave with $k_\nu^y(L_x)$ may be transmitted when crossing the QPC under consideration, we interpret $\left|t_{(\mathrm{e,o})\nu}^\mu\right|^2 k_\mu^y(a)$ as a quantity proportional to the probability of this transmission per unit time. For the energy $\mathcal{E}$, there are $\mathcal{M}(k)$ channels.

Applying conditions (6), we obtain the equations

$$N_\nu c_\nu^\mu + r_\nu^\mu = t_\nu^\mu, \qquad N_\nu c_\nu^\mu k_\nu^y(L_x) - r_\nu^\mu k_\mu^y(a) = t_\nu^\mu k_\mu^y(a).$$

Hence

$$t_\nu^\mu = N_\nu \frac{c_\nu^\mu}{2}\frac{k_\nu^y(L_x) + k_\mu^y(a)}{k_\mu^y(a)}, \qquad r_\nu^\mu = N_\nu \frac{c_\nu^\mu}{2}\frac{k_\nu^y(L_x) - k_\mu^y(a)}{k_\mu^y(a)}. \tag{27}$$

Obviously, in addition to the possibility of the transmission, the electron, when impacting upon the diaphragm with $k_\nu^y(L_x)$, may also be reflected. We stipulate that $\left|r_{(\mathrm{e,o})\nu}^\mu\right|^2 k_\mu^y(a)$ is proportional to the probability for the reflection per unit time into the μth channel. With this interpretation, we may write the alternative expression for the current $J_\nu^{(1\mathrm{e})}(k)$ in the form

$$J_\nu^{(1\mathrm{e})}(k) = -\frac{e\hbar}{m}\left[k_\nu^y(L_x) - \sum_{\mu=1}^{\mathcal{M}(k)} \left|r_\nu^\mu\right|^2 k_\mu^y(a)\right], \tag{28}$$

so that

$$k_\nu^y(L_x) = \sum_{\mu=1}^{\mathcal{M}(k)} \left|r_\nu^\mu\right|^2 k_\mu^y(a) + \sum_{\mu=1}^{\mathcal{M}(k)} \left|t_\nu^\mu\right|^2 k_\mu^y(a), \tag{29}$$

According to this balance equation, the flow $k_\nu^y(L_x)$ is ramified into $\mathcal{M}(k)$ channels both backwards and forwards. Equation (29) implies that

$$N_\nu \equiv N_\nu^{(\mathcal{M})} = \sqrt{2}\left[\sum_{\mu=1}^{\mathcal{M}(k)} \left[c_\nu^\mu\right]^2 \frac{k_\mu^y(a)^2 + k_\nu^y(L_x)^2}{k_\mu^y(a)k_\nu^y(L_x)}\right]^{-1/2}. \tag{30}$$

Thus the normalizing coefficient is channel dependent. We have indicated this fact by adding the superfix '$\mathcal{M}$' in N_ν.

3.2. *Functions* $\chi_\nu^{(1)}(\mathbf{r})$ *and* $\chi_\nu^{(2)}(\mathbf{r})$ *in the corresponding half-stripes* $y < 0$ *and* $y > 0$

For the problem that is the objective of the present paper (the conductance quantization), it is not necessary to calculate completely the wavefunctions $\chi_\nu^{(1)}(\mathbf{r})$ and $\chi_\nu^{(2)}(\mathbf{r})$ for all respective values of $y < 0$ and $y > 0$. Nevertheless, the calculation of these functions is an assignment worth in its own right. Now we will briefly show how this calculation can be implemented. We extend analytically the functions $\Omega_\nu^{(2)}(x, y)$ and $\Omega_\nu^{(1)}(x, y)$ defined by sums (19) in the whole respective half-stripes, i.e. for $x \in (-L_x/2, L_x/2)$ and, respectively, for $y < 0$ and $y > 0$. For general values of y outside the infinitesimal intervals $(-\epsilon/2, 0)$ and $(0, \epsilon/2)$, we write

$$\begin{aligned} \chi_\nu^{(2)}(x, y) &= \Omega_\nu^{(2)}(x, y) + \omega_\nu^{(2)}(x, y), \qquad y > 0, \\ \chi_\nu^{(1)}(x, y) &= \Omega_\nu^{(1)}(x, y) + \omega_\nu^{(1)}(x, y), \qquad y < 0. \end{aligned} \tag{31}$$

The corrective functions $\omega_\nu^{(\tau)}(x, y)$ have to obey simple boundary conditions. For brevity, we will confine ourselves to writing down these conditions for $\omega_\nu^{(2)}(\mathbf{r})$

$$\left.\begin{aligned}&\omega_\nu^{(2)}(x, +0) = 0\\ &\partial\omega_\nu^{(2)}(\mathbf{r})/\partial y\big|_{y=+0} = 0\end{aligned}\right\} \qquad \text{if} \quad |x| < a/2 \tag{32}$$

and

$$\left.\begin{aligned}&\omega_\nu^{(2)}(x, +0) = -\Omega_\nu^{(2)}(x, +0)\\ &\partial\omega_\nu^{(2)}(\mathbf{r})/\partial y\big|_{y=+0} = -\partial\Omega_\nu^{(2)}(\mathbf{r})/\partial y\big|_{y=+0}\end{aligned}\right\} \qquad \text{if} \quad a/2 < |x| < L_x/2. \tag{33}$$

(It is perhaps needless to emphasize that now we consider $\Omega_\nu^{(2)}(\mathbf{r})$ and $\partial\Omega_\nu^{(2)}(\mathbf{r})/\partial y$ as known functions!) We require also the fulfilment of the conditions

$$\omega_\nu^{(2)}(-a/2, y) = \omega_\nu^{(2)}(+a/2, y) = 0, \qquad y > 0. \tag{34}$$

Finally, we require that

$$\omega_\nu^{(2)}(\mathbf{r}) \to 0 \qquad \text{if} \quad y \to \infty. \tag{35}$$

Of course, $\Omega_\nu^{(2)}(\mathbf{r})$ does not tend to zero if $y \to \infty$. We may imagine the diaphragm as a source of 'radiation'. The function $\omega_\nu^{(2)}(\mathbf{r})$ could be interpreted as due to the radiation of the intervals $(-L_x/2, -a/2)$ and $(a/2, L_x/2)$ at the flanks of the window. However, an observer standing at $y = +\infty$ cannot state that only a part of the interval $(-L_x/2, L_x/2)$ radiates. This explains why the contribution of the flanks to the value of $\omega_\nu^{(2)}(\mathbf{r})$ has to approach zero if $y \to \infty$.

With boundary conditions (32)–(35), the solution $\omega_\nu^{(2)}(\mathbf{r})$ of the equation

$$\nabla^2\omega_\nu^{(2)}(\mathbf{r}) + k^2\omega_\nu^{(2)}(\mathbf{r}) = 0 \qquad \text{for} \quad -L_x/2 < x < L_x/2 \quad \text{and} \quad y > 0 \tag{36}$$

is defined completely. In order to express $\omega_\nu^{(2)}(\mathbf{r})$ explicitly, we introduce Green's function $G(\mathbf{r}|\mathbf{r}_0)$ as the solution of the equation

$$\nabla^2 G(\mathbf{r}|\mathbf{r}_0) + k^2 G(\mathbf{r}|\mathbf{r}_0) = -\delta(\mathbf{r} - \mathbf{r}_0) \qquad \text{for} \quad y \in (-\infty, +\infty), \tag{37}$$

requiring the fulfilment of the boundary conditions

$$G(-L_x/2, y|\mathbf{r}_0) = G(L_x/2, y|\mathbf{r}_0) = 0, \tag{38}$$

$$\lim_{y\to+\infty} G(\mathbf{r}|\mathbf{r}_0) = \lim_{y\to+\infty} \frac{\partial G(\mathbf{r}|\mathbf{r}_0)}{\partial y} = 0. \tag{39}$$

To satisfy condition (38), we define Green's function as the sum

$$G(\mathbf{r}|\mathbf{r}_0) = G_0(x, y|\mathbf{r}_0) + \sum_{n=1}^{\infty}(-1)^n[G_0(nL_x - x, y|\mathbf{r}_0) + G_0(nL_x + x, y|\mathbf{r}_0)]. \tag{40}$$

The function $G_0(x, y|\mathbf{r}_0)$ itself has to satisfy equation $\nabla^2 G_0 + k^2 G_0 = -\delta(\mathbf{r} - \mathbf{r}_0)$ and conditions (39). The explicit form of $G_0(x, y|\mathbf{r}_0)$ reads

$$G_0(x, y|\mathbf{r}_0) = G_0(x - x_0, y - y_0|0) = \frac{\mathrm{i}}{4}H_0^1(k\sqrt{(x - x_0)^2 + (y - y_0)^2}). \tag{41}$$

(Note that $G_0(x, y|0) = G_0(-x, y|0)$.) $H_0^1(\rho)$ is the Bessel function of the third kind known as the Hankel function, $H_0^1(\rho) = J_0(\rho) + \mathrm{i}Y_0(\rho)$. We multiply equation (36) by $G(\mathbf{r}|\mathbf{r}_0)$ and equation (37) by $\omega_\nu^2(\mathbf{r})$. Then we obtain, after exchanging the variables $\mathbf{r}$ and $\mathbf{r}_0$, the equality

$$\nabla_0.\big[G(\mathbf{r}_0|\mathbf{r})\nabla_0\omega_\nu^{(2)}(\mathbf{r}_0) - \omega_\nu^{(2)}(\mathbf{r}_0)\nabla_0 G(\mathbf{r}_0|\mathbf{r})\big] = \delta(\mathbf{r}_0 - \mathbf{r})\omega_\nu^{(2)}(\mathbf{r}_0).$$

We integrate this equality with respect to $\mathbf{r}_0$ in the upper half-stripe (i.e. for $y > 0$) between the boundaries $x = \pm L_x/2$ and employ Gauss' theorem. The result is

$$\omega_\nu^{(2)}(\mathbf{r}) = \left[\int_{-L_x/2}^{-a/2} \mathrm{d}x_0 + \int_{a/2}^{L_x/2} \mathrm{d}x_0\right] \left\{G(x_0, 0|\mathbf{r})\partial\Omega_\nu^{(2)}(\mathbf{r}_0)/\partial y_0\big|_{y_0=+0} - \Omega_\nu^{(2)}(x_0, +0)\partial G(\mathbf{r}_0|\mathbf{r})/\partial y_0\big|_{y_0=+0}\right\}. \tag{42}$$

Here we have utilized boundary conditions (32) and (33) at $y = +0$. Equation (42) is actually the direct integral formula for $\omega_\nu^{(2)}(\mathbf{r})$ and this function, when inserted in formula (31), determines the wavefunction $\psi_\nu^{(2)}(\mathbf{r})$.

Quite analogically, we can derive the function $\omega_\nu^{(1)}(\mathbf{r})$ and then, respecting formulae (14) and (31), the wavefunction $\psi_\nu^{(1)}(\mathbf{r})$ for the lower half-stripe (for $y < 0$) between the boundaries $x = \pm L_x/2$.

Above, cf formula (25), we have calculated the one-electron current $J_\nu^{(1e)}(k)$ as the current flowing just through the window at $y = +0$. However, the value of $J_\nu^{(1e)}(k)$ has to be the same even when calculated, e.g., at $y \to +\infty$. We can prove this easily. Indeed, owing to condition (35), we may state that

$$J_\nu^{(1e)}(k) = \frac{\mathrm{i}e\hbar}{2m} \lim_{y\to\infty} \int_{-L_x/2}^{L_x/2} \mathrm{d}x \left(\Omega_\nu^{(2)*}(\mathbf{r})\frac{\partial\Omega_\nu^{(2)}(\mathbf{r})}{\partial y} - \Omega_\nu^{(2)}(\mathbf{r})\frac{\partial\Omega_\nu^{(2)*}(\mathbf{r})}{\partial y}\right)$$
$$= -\frac{e\hbar}{m}\sum_{\mu=1}^{\mathcal{M}(k)} \left|t_\nu^\mu\right|^2 k_\mu^y(a). \tag{43}$$

Thus, to solve autonomously the problem formulated in subsection 3.1 has been an efficacious starting point. Afterwards, as we have shown, it is possible, if there is a need for it, to derive the solution $\psi_\nu(\mathbf{r})$ of the Schrödinger equation exactly and completely.

4. Conductance of the QPC

4.1. Derivation of the Landauer–Büttiker formula

If $k = k_\mathrm{F}$, we put the subscript 'F' in front of μ in expressions (16), (17) and (18). We assume that both the compartments in figure 1 separated by the diaphragm with the window (i.e. the leads to the window) host an ideal electron gas at $T = 0$. Since we treat the window as a QPC, our objective is to consider the non-equilibrium situation when a voltage U is applied on the QPC. We realize that if $\mathcal{E}_\mathrm{F}^{(2)} = \mathcal{E}_\mathrm{F}$ is the Fermi energy of the upper compartment, we have to consider a different value of the Fermi energy in the lower compartment, $\mathcal{E}_\mathrm{F}^{(1)} = \mathcal{E}_\mathrm{F} + eU$. We take $eU > 0$ as a small value. Then

$$k_\mathrm{F}^{(1)} = \sqrt{\frac{2m(\mathcal{E}_\mathrm{F} + eU)}{\hbar^2}} \approx \sqrt{\frac{2m\mathcal{E}_\mathrm{F}}{\hbar^2}}\left(1 + \frac{eU}{2\mathcal{E}_\mathrm{F}}\right) = k_\mathrm{F} + \frac{meU}{\hbar^2 k_\mathrm{F}},$$

where $k_\mathrm{F} = k_\mathrm{F}^{(2)} = \sqrt{2m\mathcal{E}_\mathrm{F}/\hbar^2}$. At $T = 0$, the electrons with a given energy $\mathcal{E} < \mathcal{E}_\mathrm{F}$ can be exchanged between both the compartments 1 and 2, but this does not give a contribution to the electrical current across the diaphragm. The net current is due to the electrons whose energy $\mathcal{E}$ in compartment 1 lies in the interval $(\mathcal{E}_\mathrm{F}, \mathcal{E}_\mathrm{F} + eU/(2\mathcal{E}_\mathrm{F}))$; the values of $k = \sqrt{2m\mathcal{E}/\hbar^2}$ then lie in the interval $(k_\mathrm{F}, k_\mathrm{F} + meU/(\hbar^2 k_\mathrm{F}))$. Correspondingly, if we consider the μth QPC channel in compartment 1 and use formula (18), we find that

$$k_{\mathrm{F}\mu}^{(1)}(a) = \sqrt{k_\mathrm{F}^{(1)2} - \pi^2\mu^2/a^2} = \sqrt{k_\mathrm{F}^2 - \pi^2\mu^2/a^2 + \frac{2meU}{\hbar^2}} \approx k_{\mathrm{F}\mu}^y(a) + \frac{meU}{\hbar^2 k_{\mathrm{F}\mu}^y(a)},$$

where $k^y_{\mathrm{F}\mu}(a) = \sqrt{k_{\mathrm{F}}^2 - \pi^2\mu^2/a^2}$. Hence, only few electrons can participate in the transport of charge from compartment 1 to compartment 2 employing the μth QPC channel: we have only to reckon with the electrons whose y-component $k^y_\mu(a)$ of the wave vector satisfies the inequalities

$$k^y_{\mathrm{F}\mu}(a) < k^y_\mu < k^y_{\mathrm{F}\mu}(a) + \frac{meU}{\hbar^2 k^y_{\mathrm{F}\mu}(a)}.$$

The number of allowed values of $k^y_\mu(a)$ in any interval of unit length is $1/(2\pi)$. However, an electron with a given value of $k^y_\mu(a)$ may have either spin up or spin down. Therefore, when considering the electrons in the νth state (the νth mode of the leads taken as quantum-mechanical waveguides) and in the μth QPC channel, we obtain readily their contribution to the electrical current flowing through the QPC

$$J^\mu_\nu = -\Gamma_{\mathrm{q}} U \sum_{\mu=1}^{\mathcal{M}_{\mathrm{F}}} \left|t^\mu_\nu\right|^2, \tag{44}$$

where

$$\Gamma_{\mathrm{q}} = 2e^2/h. \tag{45}$$

The transmission of electrons from compartment 1 to compartment 2 implies the negative value of the associated electrical current J^μ_ν; hence the sign minus in formula (44). The quantity Γ_{q} is the conductance quantum.

For $\mathcal{E} \to \mathcal{E}_F$, we have to consider $\mathcal{N}_{\mathrm{F}}$ waveguide modes (cf appendix A) and $\mathcal{M}_{\mathrm{F}} = \mathcal{M}(k_{\mathrm{F}})$ QPC channels. We define the conductance of the QPC as the coefficient Γ in the linear relation

$$|J| = \Gamma|U|. \tag{46}$$

In this way, we have derived the conductance of the QPC corresponding to figure 1 in the form

$$\Gamma = \Gamma_{\mathrm{q}} \sum_{\mu=1}^{\mathcal{M}_{\mathrm{F}}} \sum_{\nu=1}^{\mathcal{N}_{\mathrm{F}}} \left|t^\mu_\nu\right|^2. \tag{47}$$

This is actually the well-known Landauer–Büttiker formula [20]. However, we have not only proved the validity of this formula, in fact, we have also shown how to calculate the transmission probabilities $\left|t^\mu_\nu\right|^2$.

4.2. Conductance quantization

The integers $\mathcal{N}_{\mathrm{F}}$ and $\mathcal{M}_{\mathrm{F}}$ depend on the density n_{e} of the electrons in the leads. For a given width L_x of the leads, we prefer to use the dimensionless variable $L_x^2 n_{\mathrm{e}}$ instead of n_{e}. Then we may speak of step-like functions $\mathcal{N}_{\mathrm{F}}\left(L_x^2 n_{\mathrm{e}}\right)$, $\mathcal{M}_{\mathrm{F}}\left(L_x^2 n_{\mathrm{e}}\right)$ and, consequently, also of the step-like function $\Gamma\left(L_x^2 n_{\mathrm{e}}\right)$. However, n_{e} is a monotonous function of k_{F}, as it can be derived explicitly: see formula (A.5) of the appendix and figure 6. Instead of k_{F}, we prefer to use the dimensionless variable $u = ak_{\mathrm{F}}$. Then we may speak of step-like functions $\mathcal{N}_{\mathrm{F}}(u)$, $\mathcal{M}_{\mathrm{F}}(u)$ and, consequently, of the step-like function $\Gamma(u)$. Each jag in the curve plotted in figure 2 corresponds to the change of $\mathcal{N}_{\mathrm{F}}$ by one. On the other hand, when $\mathcal{M}_{\mathrm{F}}$ is increased by one, this corresponds to the opening of a new QPC channel.

4.2.1. Dependence of Γ *on* ak_{F}. We will now exemplify the situation choosing the width a of the QPC (i.e. the width of the gap in the diaphragm shown in figure1) equal to $L_x/2$; then $\gamma = 1/2$. As we do not consider evanescent waves in the leads, the value of k_{F} has to be

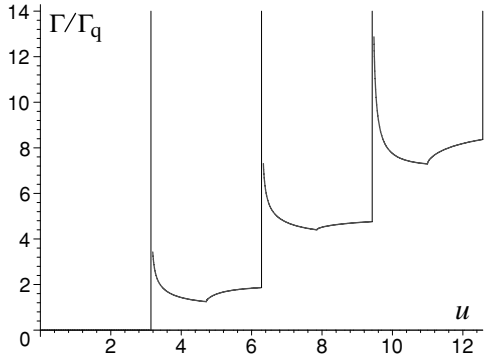

Figure 3. Dependence of the conductance Γ/Γ_q on the variable $u = ak_F$.

Table 1. Survey of lead modes, QPC channels and transmission amplitudes t_ν^μ for $\mathcal{E} < \mathcal{E}_F$ determining the conductance of the QPC for $\gamma = a/L_x = 1/2$. Table is constructed for the first two conductance steps.

Interval of u ($u = ak_F$)	$\mathcal{M}_F$ = total of active channels	$\mathcal{N}_F$ = total of of active modes	μ = serial number of channel	ν = serial number of lead mode	t_ν^μ = transmission amplitude
$(0, \pi/2)$	0	0	–	–	–
$(\pi/2, \pi)$	0	1	–	1	–
$(\pi, 3\pi/2)$	1	2	1	1	t_1^1
$(3\pi/2, 2\pi)$	1	3	1	1	t_1^1
				3	t_3^1
$(2\pi, 5\pi/2)$	2	4	1	1	t_1^1
				3	t_3^1
			2	2	t_2^2
				4	t_4^2
$(5\pi/2, 3\pi)$	2	5	–	–	–
			1	5	t_5^1

Note: For $5\pi/2 < u < 3\pi$, $\mathcal{M}_F = 2, \mathcal{N}_F = 5$, the table is the same as for $2\pi < u < 5\pi/2$, $\mathcal{M}_F = 2, \mathcal{N}_F = 4$; only the transmission amplitude t_5^1 is added

greater than π/L_x. (This may be interpreted as a manifestation of the uncertainty principle.) Consequently, it is necessary that $u = ak_F > \pi/2$ (for $\gamma = 1/2$). In tables 1 and 2, we show which values of the transmission amplitudes t_ν^μ contribute to the value of the QPC conductance. The Γ versus u plot shows that $\Gamma(u)$ is a step-like function. The positions of the edges of its steps are at $u_\mu = \pi\mu$, $\mu = 1, 2, \ldots$. The function $\Gamma(u)$ is shown in figure 3. Owing to our special choice of the gap ratio, $\gamma = 1/2$, tables 1 and 2 are relatively simple since the values of $\pi\nu/L_x$ and $\pi\mu/a$ coincide if $\nu = 2\mu$. As is seen in figure 3, the Γ versus u plot manifests jags. In general, positions of the jags are given by the values $u_\nu = \pi\nu\gamma$ ($\nu = 1, 2, \ldots$). In our case, since $\gamma = 1/2$, the jags are present only with odd integers ν. The absence of the jags if $\nu = 2j$ ($j = 1, 2, \ldots$) follows from the fact that the function $\Gamma(u)$ behaves as $A/\sqrt{u^2 - \pi^2 j^2} + B\sqrt{u^2 - \pi^2 j^2}$ (with $A > 0$, $B > 0$) if u approaches πj from the right; obviously, $B\sqrt{u^2 - \pi^2 j^2}$ is negligible in comparison with $A/\sqrt{u^2 - \pi^2 j^2}$. However, with a general value of the gap ratio $\gamma = a/L_x$ (mathematically speaking, with γ equal to an irrational number), there is no correlation between positions u_ν of jags and positions u_μ of step edges.

Sequence of transitions contributing to the value of the QPC conductance.
The diagrams correspond (from the left to the right) to increasing values of u.

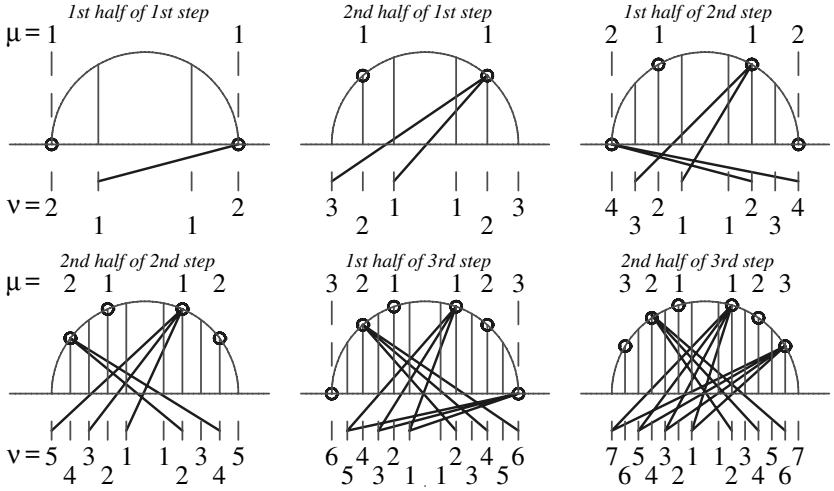

Figure 4. Diagrams corresponding to table 1 (the first four diagrams) and table 2 (the last two diagrams).

Table 2. Continuation of table 1. The table is constructed for the third conductance step. (With $\gamma = 1/2$, the table concerns $\mathcal{N}_F = 6$ and $\mathcal{N}_F = 7$.)

Interval of u ($u = ak_F$)	$\mathcal{M}_F$ = total of active channels	$\mathcal{N}_F$ = total of of active modes	μ = serial number of channel	ν = serial number of lead mode	t_ν^μ = transmission amplitude
$(3\pi, 7\pi/2)$	3	6	1	1	t_1^1
				3	t_3^1
				5	t_5^1
			2	2	t_2^2
				4	t_4^2
				6	t_6^2
			3	1	t_1^3
				3	t_3^3
				5	t_5^3
$(7\pi/2, 4\pi)$	3	7	–	–	–
			1	7	t_7^1
			3	7	t_7^3

Note: For $7\pi/2 < u < 4\pi$, $\mathcal{M}_F = 3$, $\mathcal{N}_F = 7$, the table is the same as for $3\pi < u < 7\pi/2$, $\mathcal{M}_F = 3$, $\mathcal{N}_F = 6$; only the transmission amplitudes t_7^1 and t_7^3 are added.

To make the meaning of tables 1 and 2 more apparent, we present figure 4 in which we illustrate schematically the transitions represented by the transmission coefficients t_ν^μ. Figure 4 involves six diagrams showing the upper part of the 'Fermi circle' drawn in the (k_x, k_y)-plane. (In each diagram, the horizontal axis is k_x and vertical axis is k_y. In the 2D **k**-space, the Fermi circle is the analogy to the Fermi sphere in the 3D **k**-space.) The thin vertical straight lines in the diagrams of figure 4 correspond to the lead modes. They are numbered under each semicircle. Two equal numbers mean one mode since the quantization in the x-direction is related to two opposite waves, $\exp(\mathrm{i}k_{x\nu}x)$ and $\exp(-\mathrm{i}k_{x\nu}x)$,

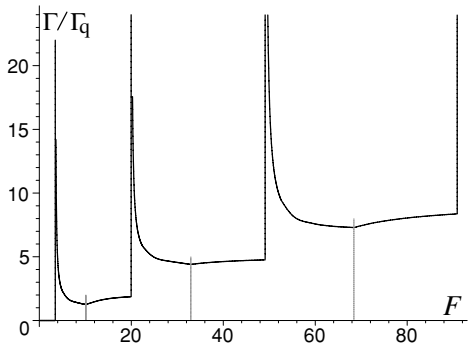

Figure 5. Dependence of the conductance Γ/Γ_q on the variable $F = L_x^2 n_e$ (and thus, for a given width L_x of the leads, on the density of electrons n_e).

where $k_{x\nu} = \pi\nu/L_x$. The little circles on the Fermi circle symbolize infinitesimal regions in the **k**-space corresponding to 'active channels'. These little circles are enumerated by the index μ. Again, two equal numbers μ (the left and the right) represent one channel. The thick straight lines drawn in the diagrams of figure 4 represent the transmission coefficients t_ν^μ. When considering these lines as arrows whose end points are the little circles, we may interpret the diagrams of figure 4 as analogues of Feynman's diagrams. (Of course, we could draw each thick line in the diagrams in four ways: the line may connect the left or right mode line with the left or right channel circle. For clarity of the graphs, we have depicted the lines from the left to the right if ν and μ are odd and from the right to the left if ν and μ are even.)

The interpretation of the diagrams of figure 4 is simple. If the gap ratio γ is kept constant, the diagrams in figure 4 illustrate the evolution of the situation with growing values of k_F. (Here a remark should be said: for convenience's sake, we depicted schematically all the Fermi circles with the same radius.) The first diagram corresponds to the process characterized by the transmission coefficient t_1^1. It is the situation when the first channel is just starting to become active. When k_F becomes greater than u_ν/a, the circles labelled by $\mu = 1$ begin moving towards the top of the Fermi circle. The second diagram shows the situation when the third mode becomes active. Then we have to consider two transmission coefficients, t_1^1 and t_3^1. In figure 3, this situation corresponds to the jag in the middle of the first conductance step. The last two diagrams correspond to the transmission coefficients involved in table 2. For instance, the sixth diagram, concerning the second half of the third step (when $7\pi/2 < u < 4\pi$), shows that the value of the conductance $\Gamma(u)$ is determined altogether by 11 coefficients t_ν^μ (eight with odd indices μ, ν and three with even indices μ, ν).

4.2.2. Dependence of Γ *on* $L_x^2 n_e$. As figure 2 clearly suggests, k_F is a monotonous function of the density n_e. Therefore, we may consider u as a well-defined function of the variable $F = L_x^2 n_e$. Correspondingly, we can depict the dependence of the conductance Γ of the QPC on the density of the electrons n_e. This dependence is shown (for $\gamma = 1/2$) in figure 5. The positions of the left edges of the three steps drawn (but also of the fourth step which is not drawn) in figure 5, $F = F_j^{\text{edge}}$, are

$$F_1^{\text{edge}} = L_x^2 n_{e1}^{\text{edge}} = 2\sqrt{3} = 3.464,$$
$$F_2^{\text{edge}} = L_x^2 n_{e2}^{\text{edge}} = 2(\sqrt{15} + \sqrt{12} + \sqrt{7}) = 19.966,$$
$$F_3^{\text{edge}} = L_x^2 n_{e3}^{\text{edge}} = 2(\sqrt{35} + \sqrt{32} + \sqrt{27} + \sqrt{20} + \sqrt{11}) = 49.116,$$
$$F_4^{\text{edge}} = L_x^2 n_{e4}^{\text{edge}} = 2(\sqrt{63} + \sqrt{60} + \sqrt{55} + \sqrt{48} + \sqrt{39} + \sqrt{28} + \sqrt{15}) = 90.874.$$

In the central part of each step, there is one jag. Positions of the jags, $F = F_j^{\mathrm{jag}}$, are

$$F_1^{\mathrm{jag}} = L_x^2 n_{\mathrm{e}1}^{\mathrm{jag}} = 2(\sqrt{8} + \sqrt{5}) = 10.129,$$
$$F_2^{\mathrm{jag}} = L_x^2 n_{\mathrm{e}2}^{\mathrm{jag}} = 2(\sqrt{24} + \sqrt{21} + \sqrt{16} + \sqrt{9}) = 32.963,$$
$$F_3^{\mathrm{jag}} = L_x^2 n_{\mathrm{e}3}^{\mathrm{jag}} = 2(\sqrt{48} + \sqrt{45} + \sqrt{40} + \sqrt{33} + \sqrt{24} + \sqrt{13}) = 68.420.$$

In the close vicinity on the right side of any value F_j^{edge}, the function $\Gamma(F)$ behaves as $\sim 1/\left(F - F_j^{\mathrm{edge}}\right)$. This behaviour corresponds to $\sim 1/\sqrt{u - j\pi}$ in the right vicinity of the value $u = j\pi$, provided that Γ is taken as a function of $u = ak_{\mathrm{F}}$. Thus, the singularities at $F = F_j^{\mathrm{edge}}$ in the plot Γ versus n_{e} are incontestable (they are even more apparent than the corresponding singularities in the plot Γ versus k_{F}). On the other hand, the presence of the jags when the conductance Γ is plotted as a function of the density n_{e} does not seem to be relevant enough. (The positions of the jags are highlighted by thin vertical straight lines in figure 5.) As is seen, the derivative $\mathrm{d}\Gamma/\mathrm{d}F$, when F approaches the value $F = F_j^{\mathrm{jag}}$ from the right, is finite, in contrast to the derivative $\mathrm{d}\Gamma/\mathrm{d}k_{\mathrm{F}}$ tending to infinity (this should particularly be manifest if figure 3 were stretched vertically) when k_{F} approaches $k_{\mathrm{F}j}^{\mathrm{jag}}$ from the right.

5. Conclusion

We can summarize the main results of this paper as follows. We have presented a detailed theory of the conductance of the quantum point contact defined by the configuration depicted in figure 1. The QPC was defined as a gap in a thin diaphragm. We have shown that it was possible to accomplish the calculation of the conductance of the QPC in an exact manner under standard simplifying conditions which were accepted previously by other authors. Here we recollect some of these conditions. The leads were deemed to be reservoirs of a 2D gas of non-interacting electrons at $T = 0$. The wavefunctions of the electrons were put equal to zero at both surfaces of the diaphragm. The conductance was calculated in the limit of a small current flowing through the QPC.

In contrast with other authors, we considered the leads to the QPC as quantum-mechanical waveguides. We employed the simplest boundary condition for the electron wavefunctions: we required that the wavefunctions have to approach zero at the boundaries of the leads. By thorough calculations, we strived to show that in case of narrow leads, it was indispensable to solve the problem of the quantization of the conductance of the QPC as a problem belonging to the theory of quantum size effects. The wavefunctions $\psi^{(0)}(\mathbf{r})$ of electrons travelling in the lead of width L_x towards the QPC have factors $\cos(\pi\nu x/L_x)$ (if ν is odd) or $\sin(\pi\nu x/L_x)$ (if ν is even). We treated ν as an index defining the electron modes in the lead. On the other hand, we paid also heed to another index, μ, enumerating 'channels' of the QPC under consideration. Namely, when $y \to 0$, the wavefunctions $\psi_\nu(\mathbf{r}) \equiv \psi_\nu(x, 0)$ in the interval $(-a/2, a/2)$ of the coordinate x (the interval defining the QPC) can be developed in the Fourier series involving $\cos(\pi\mu x/a)$ (if μ is odd) and $\sin(\pi\mu x/a)$ (if μ is even). An electron, being in mode ν and impacting upon the QPC, may employ, being transmitted through the QPC, any channel μ. These transmissions can be characterized by coefficients t_ν^μ and we showed how to calculate them exactly. Then we proved that the conductance Γ of the QPC can be expressed as a sum involving the squares of all possible coefficients t_ν^μ. Thus we actually corroborated the validity of the well-known Landauer–Büttiker formula (cf. equation (47)).

A condensed presentation of our main results has been shown in figures 3 and 5.

If the width a of the QPC is kept constant, figure 3 shows the dependence of the conductance Γ of the QPC on the Fermi momentum $\hbar k_{\mathrm{F}}$. (We preferred to use the

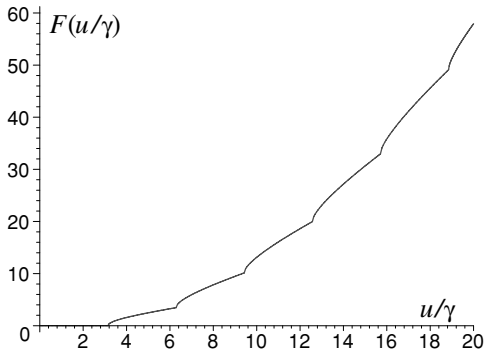

Figure 6. The first five segments (and a part of the sixth segment) of the function $F(u/\gamma)$. (The 'zeroth segment' is $F \equiv 0$.)

dimensionless variable $u = ak_{\mathrm{F}}$.) Figure 3 shows singularities that are of two kinds. First, there are the singularities of the type $\sim 1/\sqrt{u - u_j^{\mathrm{edge}}}$ $\left(u > u_j^{\mathrm{edge}}\right)$ at the frontal edges of the conductance steps; second, there are the jags, corresponding to the behaviour of Γ of the type $\sim\sqrt{u - u_j^{\mathrm{jag}}}$ after the jag points $\left(u > u_j^{\mathrm{jag}}\right)$. The jags stem from the waveguide character of the leads. As we have elucidated particularly in subsection 4.2, there is no difficulty to comprehend their origin. Since $k_{\mathrm{F}} = \sqrt{2m\mathcal{E}_{\mathrm{F}}}/\hbar$, the plot shown in figure 3 can be transformed into a similar plot illustrating the dependence of Γ on the Fermi energy $\mathcal{E}_{\mathrm{F}}(k_{\mathrm{F}})$, with the same singularities as those shown in figure 3. Although the singularities of the type $\sim 1/\sqrt{\mathcal{E}_{\mathrm{F}} - \mathcal{E}_{\mathrm{F}}\left(u_j^{\mathrm{edge}}\right)}$ seem to be strange at first sight, we emphasize that their presence in the conductance versus $\mathcal{E}_{\mathrm{F}}$ plot is in no contradiction with the Landauer–Büttiker formula which has been, as we have proved above, confirmed unequivocally by our theory. In fact, we have recently derived singularities of this type also in the dependence of the conductance of 3D Sharvin contacts on the Fermi energy [21]. These singularities resemble the Van Hove singularities known in the theory of the density of states of quasi-particles [22].

In figure 5, which is the direct equivalent of figure 3, we have illustrated the dependence of Γ on the density n_{e} of the electrons. (In fact, not the Fermi energy or the Fermi momentum, but the density n_{e} is controlled primarily in experiments.) If $n_{\mathrm{e}j}^{\mathrm{edge}}$ is the value of n_{e} corresponding to $u = u_j^{\mathrm{edge}}$, the singular behaviour of the function $\Gamma(n_{\mathrm{e}})$ on the right side of $n_{\mathrm{e}j}^{\mathrm{edge}}$ is of the type $\sim 1/\left(n_{\mathrm{e}} - n_{\mathrm{e}j}^{\mathrm{edge}}\right)$.

The singular behaviour of the coefficients t_ν^μ as functions of the variable u is neither dictated nor prohibited by the Landauer–Büttiker formula. Nothing else than the Schrödinger equation is responsible for it. The singular behaviour of the function $t_\nu^\mu(u)$ if u approaches $u_\mu \equiv u_j^{\mathrm{edge}}$ from the right can be interpreted as a resonance phenomenon: at the resonant condition when $u = u_j^{\mathrm{edge}}$, the QPC is ideally transparent for the electrons. The infinite conductance Γ means the zero intrinsic resistance $R_{\mathrm{QPC}} = 1/\Gamma$ of the QPC. However, the resistance R_{QPC} is in series with the resistance of the leads, R_{leads}. Therefore, the total resistance of the system 'QPC + leads' is $R_{\mathrm{total}} = R_{\mathrm{QPC}} + R_{\mathrm{leads}}$. If $R_{\mathrm{QPC}} \to +0$ at $u = u_j^{\mathrm{edge}}$, this means that when measuring the resistance of the point contact, one measures actually the resistance of the leads. At the resonant condition $u = u_j^{\mathrm{edge}}$, the conductance $\Gamma_{\mathrm{total}} = 1/R_{\mathrm{total}}$ is finite, although may be high enough in comparison with values of the conductance of the QPC at non-resonant values of u.

Thus, we predict that the conductance of QPCs in Γ versus n_e (or Γ versus $\mathcal{E}_F$) plots should disclose well detectable maxima at the frontal edges of the conductance steps. At present, however, we are not aware of any measurements supporting this prediction. We hope that there is no serious impediment to carry out such measurements.

Acknowledgments

This work has been supported by the Slovak Research and Development Agency under the contract APVV-51-003505 and by the Grant Agency VEGA of the Slovak Academy of Sciences and the Ministry of Education of the Slovak Republic under contract 1/0096/08.

Appendix A. Dependence of the density of electrons n_e on the variable k_F

We will now consider values of $k_\nu^y(L_x)$ for which $\mathcal{E} < \mathcal{E}_F$. Let $\mathcal{N}_F \geqslant 1$ be the maximum value of the index ν for which $k_F > \pi\mathcal{N}_F/L_x$. If $1 \leqslant \nu \leqslant \mathcal{N}_F$, the electrons can travel as waves $\sim \exp\left(\pm i k_\nu^y(L_x) y\right)$ in the y-direction, with $k_\nu^y(L_x) < k_{F,\nu}^y(L_x)$. (Cf definition (11).) Following the standard way of derivation, we write the equality

$$\frac{1}{\pi}\int_{-k_{F,1}^y(L_x)}^{k_{F,1}^y(L_x)} \mathrm{d}k_y = \frac{2}{\pi}k_{F,1}^y(L_x) = \frac{2}{\pi}\sqrt{k_F^2 - \left(\frac{\pi}{L_x}\right)^2} = L_x n_e, \qquad \frac{\pi}{L_x} < k_F < \frac{2\pi}{L_x}. \tag{A.1}$$

Similarly,

$$\frac{2}{\pi}\left[\sqrt{k_F^2 - \left(\frac{\pi}{L_x}\right)^2} + \sqrt{k_F^2 - \left(\frac{2\pi}{L_x}\right)^2}\right] = L_x n_e, \qquad \frac{2\pi}{L_x} < k_F < \frac{3\pi}{L_x}, \tag{A.2}$$

etc. After multiplying equations (A.1) and (A.2) by a, we introduce the dimensionless quantity $\gamma = a/L_x$ and define, for the variable

$$u/\gamma = L_x k_F, \tag{A.3}$$

the function

$$F(u/\gamma) = L_x^2 n_e. \tag{A.4}$$

Then, using the Heaviside function $\Theta(\xi)$, we may write

$$\begin{aligned} F(u/\gamma) = \frac{2}{\pi}[&\sqrt{(u/\gamma)^2 - \pi^2}\Theta(u/\gamma - \pi) + \sqrt{(u/\gamma)^2 - (2\pi)^2}\Theta(u/\gamma - 2\pi) \\ &+ \cdots + \sqrt{(u/\gamma)^2 - (\mathcal{N}_F\pi)^2}\Theta(u/\gamma - \mathcal{N}_F\pi)] \end{aligned} \tag{A.5}$$

for $u < (\mathcal{N}_F + 1)\pi\gamma$. The plot of this function is shown in figure 6.

Let $F_j^{\max}$ be the maximum value of $F(u/\gamma)$ for the j th segment

$$\begin{aligned} F_1^{\max} &= 2\sqrt{3}, \\ F_2^{\max} &= 2(\sqrt{8} + \sqrt{5}), \\ &\cdots \\ F_{\mathcal{N}_F}^{\max} &= 2\left(\sqrt{(\mathcal{N}_F + 1)^2 - 1} + \sqrt{(\mathcal{N}_F + 1)^2 - 4} + \cdots + \sqrt{(\mathcal{N}_F + 1)^2 - \mathcal{N}_F^2}\right). \end{aligned} \tag{A.6}$$

If the value of $\mathcal{N}_F$ is high, this means that the stripe under consideration is wide. We may then take the replacements $F_{\mathcal{N}_F}^{\max} \approx F_{\mathcal{N}_F-1}^{\max} \to L_x^2 n_e, \mathcal{N}_F \to L_x k_F/\pi$. When introducing a

continuous surrogate variable t instead of $\nu/\mathcal{N}_\mathrm{F}$ and when considering $1/\mathcal{N}_\mathrm{F}$ as $\mathrm{d}t$, we may utilize the approximation

$$F^{\max}_{\mathcal{N}_\mathrm{F}-1} = 2\mathcal{N}_\mathrm{F}^2 \sum_{\nu=1}^{\mathcal{N}_\mathrm{F}-1} \frac{1}{\mathcal{N}_\mathrm{F}}\sqrt{1-\nu^2/\mathcal{N}_\mathrm{F}^2} \to L_x^2 n_\mathrm{e} \approx 2\left(\frac{L_x k_\mathrm{F}}{\pi}\right)^2 \int_0^1 \mathrm{d}t\sqrt{1-t^2} = \frac{L_x^2 k_\mathrm{F}^2}{2\pi}.$$

Thus, in the limit of wide stripes, we obtain the parabolic dependence

$$n_\mathrm{e} \approx \frac{k_\mathrm{F}^2}{2\pi}. \tag{A.7}$$

The curve in figure 6 follows manifestly this parabola. It is interesting that in spite of the positive second derivative $\mathrm{d}^2 n_\mathrm{e}/\mathrm{d}k_\mathrm{F}^2$ in the limit of wide stripes (namely $\mathrm{d}^2 k_\mathrm{F}^2/\mathrm{d}k_\mathrm{F}^2 = 2$), the second derivative $\mathrm{d}^2 n_\mathrm{e}/\mathrm{d}k_\mathrm{F}^2 \sim \mathrm{d}^2 F/\mathrm{d}u^2$ of each segment of the function plotted in figure 6 is negative!

It is easy to invert formulae (A.1) and (A.2)

$$\frac{\pi}{L_x} < k_\mathrm{F} = \frac{\pi}{L_x}\sqrt{1+\left(\frac{L_x^2 n_\mathrm{e}}{2}\right)^2} < \frac{2\pi}{L_x}, \tag{A.8}$$

$$\frac{2\pi}{L_x} < k_\mathrm{F} = \frac{\pi}{L_x}\sqrt{\left(\frac{L_x^2 n_\mathrm{e}}{4} - \frac{3}{L_x^2 n_\mathrm{e}}\right)^2 + 4} < \frac{3\pi}{L_x}. \tag{A.9}$$

When using the dimensionless quantities u and γ, we can rewrite these formulae as

$$u/\gamma = \pi\sqrt{1+F^2/4} \qquad \text{if} \quad 0 < F < F_1^{\max}, \tag{A.10}$$

$$u/\gamma = \pi\sqrt{(F/4 - 3/F)^2 + 4} \qquad \text{if} \quad F_1^{\max} < F < F_2^{\max}. \tag{A.11}$$

To express analytically the dependence of u/γ on F is difficult if $F > F_2^{\max}$. Nevertheless, from a graphical viewpoint, the problem of displaying u/γ versus F plot is essentially reduced to exchanging the axes in figure 6. In this way, we have obtained figure 2 showing the dependence of u/γ on F.

Appendix B. Calculation of transmission amplitudes for the first three conductance steps

For the gap ratio $\gamma = 1/2$, we obtain, according to formulae (22), the factors

$$\left[c_1^1\right]^2 = 64/9, \qquad \left[c_3^1\right]^2 = 64/25, \qquad \left[c_5^1\right]^2 = 64/441, \qquad \left[c_7^1\right]^2 = 64/2025, \tag{B.1}$$

$$\left[c_2^2\right]^2 = 32/9, \qquad \left[c_4^2\right]^2 = \pi^2/2, \qquad \left[c_6^2\right]^2 = 32/25, \tag{B.2}$$

$$\left[c_3^1\right]^2 = 576/1225, \qquad \left[c_3^3\right]^2 = 64/81, \qquad \left[c_5^3\right]^2 = 576/121, \qquad \left[c_7^3\right]^2 = 576/169. \tag{B.3}$$

In the first of formulae (27), there is the factor

$$\frac{k_\nu^y(L_x) + k_\mu^y(a)}{k_\mu^y(a)} = 1 + \sqrt{\frac{u^2 - \pi^2\gamma^2\nu^2}{u^2 - \pi^2\mu^2}}. \tag{B.4}$$

The terms in the sum in formula (30) are proportional to

$$\frac{k_\mu^y(a)^2 + k_\nu^y(L_x)^2}{k_\mu^y(a)k_\nu^y(L_x)} = \frac{2u^2 - \pi^2(\mu^2+\gamma^2\nu^2)}{\sqrt{(u^2-\pi^2\mu^2)(u^2-\pi^2\gamma^2\nu^2)}}. \tag{B.5}$$

We present some relevant squares of the normalization coefficients for $\gamma \to 1/2$

$$\begin{cases} \left[N_1^{(1)}\right]^2 = \frac{2}{[c_1^1]^2}\frac{\sqrt{(u^2-\pi^2)(u^2-\pi^2\gamma^2)}}{2u^2-\pi^2(1+\gamma^2)} & \to \frac{9}{32}\frac{\sqrt{(u^2-\pi^2)(u^2-\pi^2/4)}}{2u^2-5\pi^2/4}, \\ \left[N_3^{(1)}\right]^2 = \frac{2}{\left[c_3^1\right]^2}\frac{\sqrt{(u^2-\pi^2)(u^2-9\pi^2\gamma^2)}}{2u^2-\pi^2(1+9\gamma^2)} & \to \frac{25}{32}\frac{\sqrt{(u^2-\pi^2)(u^2-9\pi^2/4)}}{2u^2-13\pi^2/4}, \\ \left[N_5^{(1)}\right]^2 = \frac{2}{\left[c_5^1\right]^2}\frac{\sqrt{(u^2-\pi^2)(u^2-25\pi^2\gamma^2)}}{2u^2-\pi^2(1+25\gamma^2)} & \to \frac{441}{32}\frac{\sqrt{(u^2-\pi^2)(u^2-25\pi^2/4)}}{2u^2-29\pi^2/4}, \\ \left[N_7^{(1)}\right]^2 = \frac{2}{\left[c_7^1\right]^2}\frac{\sqrt{(u^2-\pi^2)(u^2-49\pi^2\gamma^2)}}{2u^2-\pi^2(1+49\gamma^2)} & \to \frac{2025}{32}\frac{\sqrt{(u^2-\pi^2)(u^2-49\pi^2/4)}}{2u^2-53\pi^2/4}, \end{cases} \tag{B.6}$$

$$\begin{cases} \left[N_2^{(2)}\right]^2 = \frac{2}{\left[c_2^2\right]^2}\frac{\sqrt{(u^2-4\pi^2)(u^2-4\pi^2\gamma^2)}}{2u^2-4\pi^2(1+\gamma^2)} & \to \frac{9}{16}\frac{\sqrt{(u^2-4\pi^2)(u^2-\pi^2)}}{2u^2-5\pi^2}, \\ \left[N_4^{(2)}\right]^2 = \frac{2}{\left[c_4^2\right]^2}\frac{\sqrt{(u^2-4\pi^2)(u^2-16\pi^2\gamma^2)}}{2u^2-4\pi^2(1+4\gamma^2)} & \to \frac{4}{\pi^2}, \\ \left[N_6^{(2)}\right]^2 = \frac{2}{\left[c_6^2\right]^2}\frac{\sqrt{(u^2-4\pi^2)(u^2-36\pi^2\gamma^2)}}{2u^2-4\pi^2(1+9\gamma^2)} & \to \frac{25}{16}\frac{\sqrt{(u^2-4\pi^2)(u^2-9\pi^2)}}{2u^2-13\pi^2}, \end{cases} \tag{B.7}$$

$$\begin{cases} \left[N_1^{(3)}\right]^2 = 2\Big[\left[c_1^1\right]^2\frac{2u^2-\pi^2(1+\gamma^2)}{\sqrt{(u^2-\pi^2)(u^2-\pi^2\gamma^2)}} + \left[c_1^3\right]^2\frac{2u^2-\pi^2(9+\gamma^2)}{\sqrt{(u^2-9\pi^2)(u^2-\pi^2\gamma^2)}}\Big]^{-1} \\ \quad \to \frac{\sqrt{u^2-\pi^2/4}}{32}\Big[\frac{1}{9}\frac{2u^2-5\pi^2/4}{\sqrt{u^2-\pi^2}} + \frac{9}{1225}\frac{2u^2-13\pi^2/4}{\sqrt{u^2-9\pi^2}}\Big]^{-1}, \\ \left[N_3^{(3)}\right]^2 = 2\Big[\left[c_1^1\right]^2\frac{2u^2-\pi^2(1+9\gamma^2)}{\sqrt{(u^2-\pi^2)(u^2-9\pi^2\gamma^2)}} + \left[c_3^3\right]^2\frac{2u^2-9\pi^2(1+\gamma^2)}{\sqrt{(u^2-9\pi^2)(u^2-9\pi^2\gamma^2)}}\Big]^{-1} \\ \quad \to \frac{\sqrt{u^2-9\pi^2/4}}{32}\Big[\frac{1}{25}\frac{2u^2-13\pi^2/4}{\sqrt{u^2-\pi^2}} + \frac{1}{81}\frac{2u^2-45\pi^2/4}{\sqrt{u^2-9\pi^2}}\Big]^{-1}, \\ \left[N_5^{(3)}\right]^2 = 2\Big[\left[c_5^1\right]^2\frac{2u^2-\pi^2(1+25\gamma^2)}{\sqrt{(u^2-\pi^2)(u^2-25\pi^2\gamma^2)}} + \left[c_5^3\right]^2\frac{2u^2-\pi^2(9+25\gamma^2)}{\sqrt{(u^2-9\pi^2)(u^2-25\pi^2\gamma^2)}}\Big]^{-1} \\ \quad \to \frac{\sqrt{u^2-25\pi^2/4}}{32}\Big[\frac{1}{441}\frac{2u^2-29\pi^2/4}{\sqrt{u^2-\pi^2}} + \frac{9}{121}\frac{2u^2-61\pi^2/4}{\sqrt{u^2-9\pi^2}}\Big]^{-1}, \\ \left[N_7^{(3)}\right]^2 = 2\Big[\left[c_7^1\right]^2\frac{2u^2-\pi^2(1+49\gamma^2)}{\sqrt{(u^2-\pi^2)(u^2-49\pi^2\gamma^2)}} + \left[c_7^3\right]^2\frac{2u^2-\pi^2(9+49\gamma^2)}{\sqrt{(u^2-9\pi^2)(u^2-49\pi^2\gamma^2)}}\Big]^{-1} \\ \quad \to \frac{\sqrt{u^2-49\pi^2/4}}{32}\Big[\frac{1}{2025}\frac{2u^2-53\pi^2/4}{\sqrt{u^2-\pi^2}} + \frac{9}{169}\frac{2u^2-85\pi^2/4}{\sqrt{u^2-9\pi^2}}\Big]^{-1}. \end{cases} \tag{B.8}$$

Let us now present two final expressions. First, we present the dependence of $\left|t_1^1\right|^2$ on u for $\gamma \to 1/2$

$$\left|t_1^1\right|^2 = \frac{\left[N_1^{(1)}\right]^2\left[c_1^1\right]^2}{4}\left(\frac{k_1^y(a)+k_1^y(L_x)}{k_1^y(a)}\right)^2 \to \frac{1}{2}\frac{\sqrt{u^2-\pi^2/4}(\sqrt{u^2-\pi^2/4}+\sqrt{u^2-\pi^2})^2}{\sqrt{u^2-\pi^2}(2u^2-5\pi^2/4)}. \tag{B.9}$$

Clearly, the function $\left|t_1^1\right|^2$ behaves as $\sim 1/\sqrt{u^2-\pi^2}$ if u goes to π from the right. This is the behaviour at the edge of the first step shown in figure 3. Second,

$$|t_3^1|^2 = \frac{\left[N_3^{(1)}\right]^2\left[c_3^1\right]^2}{4}\left(\frac{k_1^y(a)+k_3^y(L_x)}{k_1^y(a)}\right)^2$$
$$\to \frac{1}{2\sqrt{u^2-\pi^2}}\left[\sqrt{u^2-\pi^2/4}\frac{(\sqrt{u^2-\pi^2/4}+\sqrt{u^2-\pi^2})^2}{2u^2-5\pi^2/4}\right.$$
$$\left.+\sqrt{u^2-9\pi^2/4}\frac{(\sqrt{u^2-\pi^2}+\sqrt{u^2-9\pi^2/4})^2}{2u^2-13\pi^2/4}\right]. \qquad \text{(B.10)}$$

This expression manifests the behaviour of the function $|t_3^1|^2$ of the type $\sim$(const + $\sqrt{u^2-9\pi^2/4}$) if u goes to $3\pi/2$ from the right, i.e. the behaviour at the jag of the first conductance step in figure 3.

References

[1] Ziman J M 1960 *Electrons and Phonons* (Oxford: Oxford University Press)
[2] Sandomirskii B V 1967 *Sov. Phys.—JETP* **25** 101
[3] Bezák V 1966 *J. Phys. Chem. Solids* **27** 815
[4] Bezák V 1966 *J. Phys. Chem. Solids* **27** 821
[5] Ando T 1982 A. B. Fowler, F. Stern *Revs. Mod. Phys.* **54** 437
[6] van Wees B J, van Houten H, Beenakker C W J, Williamson J G, Kouwenhoven L P, van der Marel D and Foxon C T 1988 *Phys. Rev. Lett.* **60** 848
[7] Wharam D A, Thornton T J, Newbury R, Pepper M, Ahmed H, Frost J E F, Hasko D G, Peacock D C, Ritchie D A and Jones G A C 1988 *J. Phys. C: Solid State Phys.* **21** L209
[8] Haanappel E G and van der Marel D 1988 *Phys. Rev.* B **39** 5484
[9] Avishai Y and Band Y B 1989 *Phys. Rev.* B **40** 12535
[10] Kirczenow G 1989 *Phys. Rev.* B **39** 10452
[11] Matulis A and Šegžda D 1989 *J. Phys.: Condens. Matter* **1** 2289
[12] Szafer A and Stone A D 1989 *Phys. Rev. Lett.* **62** 300
[13] Berggren K-F and Li Ji Z 1990 *Phys. Rev.* B **43** 4760
[14] Tekman E and Ciraci S 1990 *Phys. Rev.* B **42** 9098
[15] Beenakker C W J and van Houten H 1991 *Solid State Phys.* **44** 1
[16] Tekman E and Ciraci S 1991 *Phys. Rev.* B **43** 7145
[17] Nikolić B and Allen P B 1999 *Phys. Rev.* B **60** 3963
[18] Lal S, Rao S and Sen D 2002 *Phys. Rev.* B **65** 195304
[19] Dacal L C O, Damião Á J and de Andrada e Silva E A 2005 *Phys. Rev.* B **71** 155330
[20] Datta S 1995 *Electronic Transport in Mesoscopic Systems* (Cambridge: Cambridge University Press)
[21] Bezák V 2007 *Ann. Phys., NY* **322** 2603
[22] March N H, Young W H and Sampanthar S 1967 *The Many-Body Problem in Quantum Mechanics* (Cambridge: Cambridge University Press)